Structure and crystal growth approach of poly(alkylacrylate) myelinic vesicles by electron microscopy

S. Giorgio and R. Kern
CRMC2-CNRS, Campus de Luminy, case 913, 13288 Marseille Cedex 09, France
(Received 30 May 1984; revised 27 September 1984)

Alkylacrylate copolymers $[-CH_2-\underset{|}{CH}-COO-C_{22}H_{45}]_n$ form a myelinic phase showing vesicles ~1000 Å in diameter and a minimum thickness of 30 Å. Electron microscope and diffraction patterns show that the membrane is a monolayer of the hexagonal stacking of the C_{22} alkyl chains. A structural model is proposed showing how the alkylchains are connected by the principal polymer chain. The growth mechanism of such vesicles is discussed.

(Keywords: alkylacrylate copolymer; vesicles; structure; electron microscopy; crystal growth)

INTRODUCTION

The myelinic figures first observed by Virchow in 1854 on mixing lecithin and water, belong to the different varieties of lamellar mesomorphic phases. The best defined lecithin–water system has been studied in detail by Nageotte[1] in 1937. More recently, Saupe[2] discussed this system and gave a stability analysis of these mobile figures. Optical studies suggest that the lamellar mesophase forms concentric hollow cylinders as long as a concentration gradient of the solvent within the lamella exists. The hollow mobile tube bends and undergoes periodic strictions, so that a string of beads is formed. The spherical vesicles remain connected by tiny tubes as long as there is no outside disturbance.

Recently, Wittmann *et al.*[3] showed that the myelinic figures can also be produced in non-amphiphilic systems such as the block copolymer polystyrene–polyisoprene. These authors propose a rule for preparing myelinic figures. The block polymer has to be dissolved or swelled in a first solvent in order to mobilize both sequences of the polymer, then a second solvent has to be carefully added. This second solvent must be highly specific to only one of the sequences.

The study of myelinic phases probably has some biological interest as model membranes. Therefore, some additional information concerning their molecular structure is desirable. Myelinic phases may have also some industrial interest in several crystallization processes. During the study of just such a type of problem we found[4] that copolymers of alkyl acrylate form myelinic vesicles and have specific seeding effects on supersaturated solutions of normal paraffins; we will report elsewhere about this type of application.

Whatever our motivation, we could produce very small vesicles (~1000Å) of alkyl–acrylate and therefore study them by electron microscopy and microdiffraction. These vesicles gave good electron diffraction patterns thus dark field imaging techniques could be used and finally a structural model of the vesicles and a growth mechanism proposed.

CHARACTERIZATION OF THE COPOLYMER

The copolymer used is an alkyl–acrylate commercially termed Shell dewaxing aid 1615, of general formula:

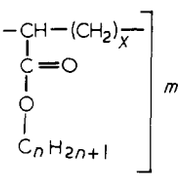

The elementary analysis gives:
C:78.9%, H = 12.6%, O = 8.5%, in weight per cent, so that $x+n=23$. Saponification of the esters, followed by gas chromatography of the alkyl groups gives $n=22$. The method was tested on poly(dodecylacrylate) and poly(octadecylmethacrylate) kindly donated by Prof. Vallet (Lyon).

A ^{13}C n.m.r. analysis confirmed that this polymer is an acrylate and not a methacrylate and furthermore that there are 3.9 esters groups per 100 carbon atoms, so that $n=22$. Therefore, only one CH_2 group, $x=1$, separates two neighbouring substituted carbons along the principal chain. Gel permeation measurements showed a large dispersion in the principal chain length, the molecular weights have a maximum at 8×10^4 but ranging from 1×10^4 to 5×10^6.

SAMPLE PREPARATION AND BRIGHT FIELD OBSERVATION OF THE MYELINIC FIGURES

The copolymer is dissolved at 0.3% in toluene at 60°C. Heptan at 60°C is added to this solution in a volumic ratio of 95/5. No special care is taken during the mixing while a magnetic stirrer is at work. The solution remains

0032-3861/85/060837-11$03.00

transparent but illumination with laser light shows strong diffusion occurring. An electron microscope grid, covered with a carbon film is dipped in this solution and the remaining solvent is then removed by capillarity.

This grid is observed in bright field illumination in a JEOL 100 C TEM at the magnification $G = 1.10^5$–6.10^5 with irradiations of 10–400 C $s^{-1}.cm^{-2}$. Exposure time $t = 5$–10 s. Cylindrical shaped particles can be observed (*Figure 1a*), some of them presenting pseudoperiodic diameter variations (*Figure 1b*). Isolated spheres (*Figures 1c*) with diameters varying between 200–3000 Å are also observed. Particles also seem to form strings of beads (*Figure 1d*). These are typical morphological aspects observed on myelinic figures. The method of preparation we used is quite the same as the method used by Wittmann *et al.*[3] for the copolymer polystyrene–polyisoprene. It satisfies also the rule these authors proposed, toluene being a solvent of both the alkylgroups and the ester groups. The second solvent we used, heptan, is only a good solvent for the alkyl chains.

In solution it is probable that the described particles contain solvent and in the TEM vacuum the particles dry out and crush against the carbon support and eventually fold upon themselves. All crushed particles show a peripheral edge with a minimum thickness of 30 Å. Upon crushing, multiple folding occurs, several border lines are seen (*Figure 1b*) and the edge is then thicker. The string of beads and the isolated spheres show the edges of minimal thickness (*Figure 1c* and *d*). Some of the smallest crushed spheroids display straight edges and some have polygonal shape. All these aspects confirm the idea that these particles are close vesicles 30 Å thick.

Even in the bright field illumination some contrast can be observed (*Figure 1b*) on the surface of the vesicles in the form of a mosaic of irregular but adjacent patches (50–100 Å in diameter). The edges of the vesicles show also a striation contrast normal to the outline (*Figure 1b*). We will come back to this point later.

ELECTRON DIFFRACTION PATTERNS

One of the most surprising facts discovered was that the crushed vesicles with cylindrical and spherical shapes gave good electron diffraction patterns, nothing except the observed contrast in the bright field illumination (see previous section) could allow us to suppose that. The resistance against irradiation of the vesicles is high. By measuring the vanishing of the diffraction patterns, a critical dose $D_c = 1 \times 10^4$–2×10^4 C/m^2 can be determined.

Debye-Scherrer patterns

When working in the diffraction mode with TEM, a single vesicle exhibits dotted Debye–Scherrer rings (*Figure 2*). In *Table 1* the corresponding spacings of the five successive rings observed are given. They can be indexed by *hko* considering a two dimensionnal lattice with parameters $a = b = 4.8$ Å and $\gamma = 120°$. These

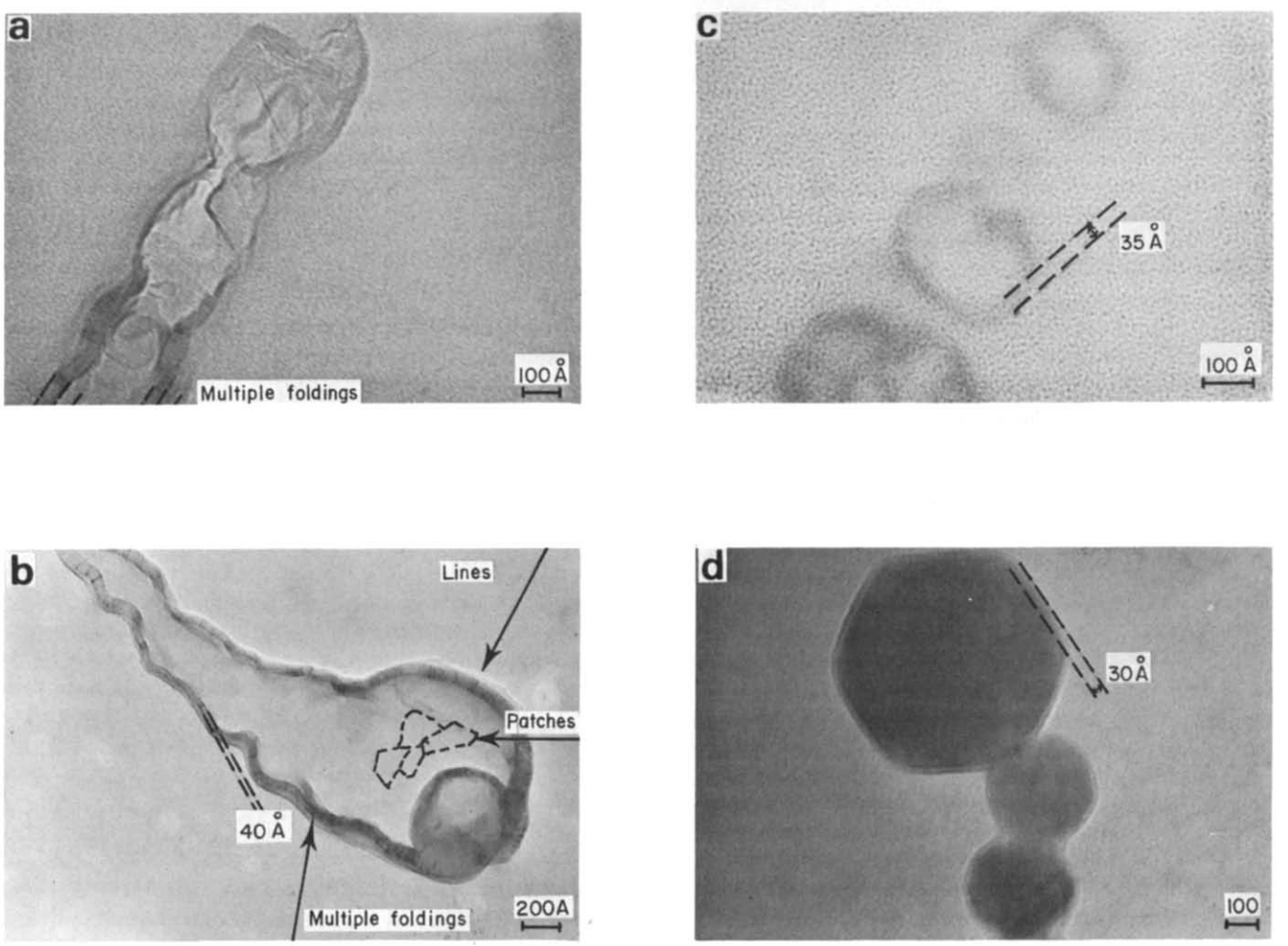

Figure 1 a,b,c,d: crushed cylindrical and spherical shaped vesicles of C_{22} polyalkylacrylate

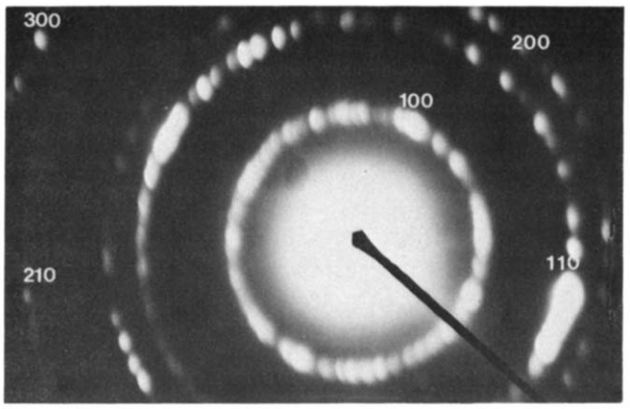

Figure 2 Debye Scherrer pattern with five reflections (*hko*) of a typical hexagonal paraffin structure, obtained with vesicles of *Figure 1*

Table 1 Two dimensional lattice spacings of the five Debye–Scherrer rings exhibited by a single vesicle

d(Å)	4.15	2.4	2.07	1.57	1.04
hko	100	110	200	210	220 300

parameters are close to those for normal hexagonal paraffin crystals.

An interesting fact is that these Debye–Scherrer patterns do not remain circular when the vesicles are tilted on the goniometer stage towards the electron beam at an angle α. The circles become ellipses, the small axis of the ellipses having the same values as the circle diameters, but the great axis increases as $1/\cos\alpha$. This is a clear indication that in the reciprocal space there are spikes along [001]* and that the structure is not perfectly tridimensional but has some twodimensional character. We will come back to this point later.

Microdiffraction patterns: dark field images

Intensities of 15 C/s m^2 were used at magnification $G=3\times10^5$. An electron beam of aperture 0.2 μm was used and selected area diffraction patterns could be obtained on different parts of the vesicles. Schematically in *Figure 3a* the aperture covers the entire vesicle, in *Figure 3b* only the edge of a vesicle was selected. In *Figure 3c* there is no edge present on one side of a vesicle. Here the membrane has locally just one thickness and a single crystal pattern can be obtained (*Figure 4c*). This pattern displays the *hko* reflections of the reciprocal plane (001)* that would be produced by normal hexagonal paraffin structure with $a=4.8$ Å. Such patterns are due to the diffraction of a single patch. When several patches contribute to the diffraction (*Figure 3a*) the pattern is that of *Figure 4a* where all the spots can be indexed as (*hko*) reflections of such (001)* planes but in azimuthal disorder. The membrane is therefore formed by several monocrystalline patches mutually misoriented as in an azimuthal powder texture.

In order to confirm this point, dark field images have been taken on a string of crushed vesicles as seen in *Figure 5a* (bright field). A 40 μm aperture has been used for selecting a section of the spots of the 110 Debye–Scherrer ring. The resulting image (*Figure 5b*) shows patches illuminated on the surface of the vesicle as well on the edges and multiple folded parts inside the vesicle. The monocrystalline domains 50–100 Å in diameter correspond to patches seen in some bright field images (*Figure 1b*).

When the edge of a vesicle is selected as schematically shown in *Figure 3b* and the useful part of this edge is fairly straight, the diffraction pattern is that of *Figure 4b* where three even reflections of a reciprocal row |*kho*|* can be seen; a row which is always parallel to the edge of the vesicle. This pattern corresponds to a line grating of spacing 2.4 Å, parallel to the striations in the edge observed in the bright field images (*Figure 1b*). This periodicity may correspond to a stacking of paraffin chains lying on the substrate in (110) planes normal to the substrate. These paraffin chains exhibit a disorder parallel to the chains since the reciprocal space is that corresponding to a line grating. Therefore the thickness of the edge should be the length of the alkyl chain of 22 carbon atoms. In bright field illumination the thickness of the edge, ~30 Å, confirms this point.

Paracrystalline disorder

All the diffraction patterns (001)* observed exhibit large spots with an integral breath of $10^{-1}<\beta<10^{-2}$ Å^{-1} somewhat higher than the instrumental broadening β_i we measured that is $\beta_i=8\times10^{-3}$ Å^{-1}. This broadening is due in part to the limited number N_a of lattice cells in the monocrystalline domains (patches), since these domains contain $N_a=10$–20 cells along a linear dimension. This finite size effect leads to an integral broadening of

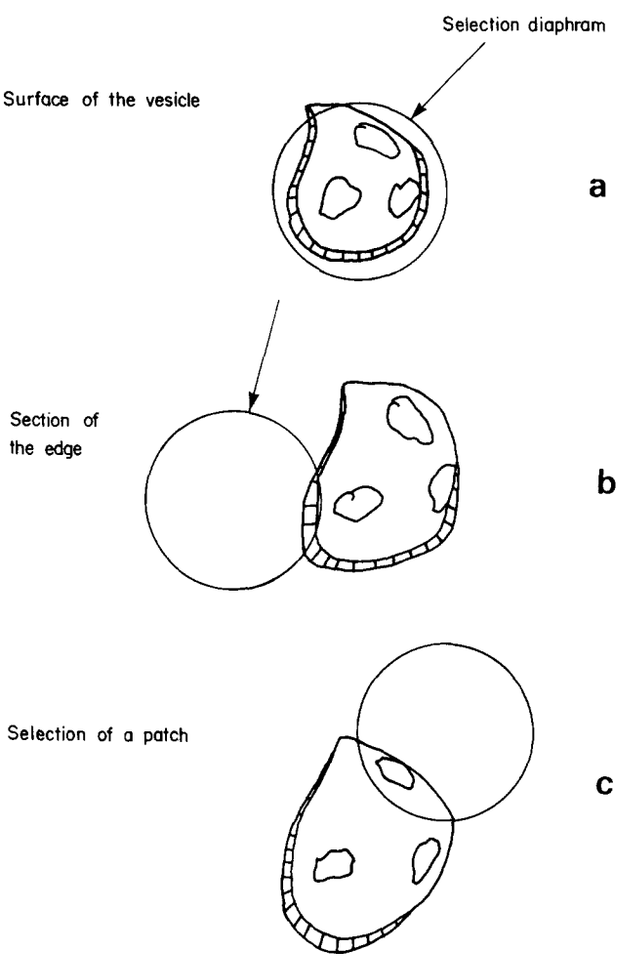

Figure 3 a,b,c: position of the selection diaphragm with respect to different parts of a vesicle

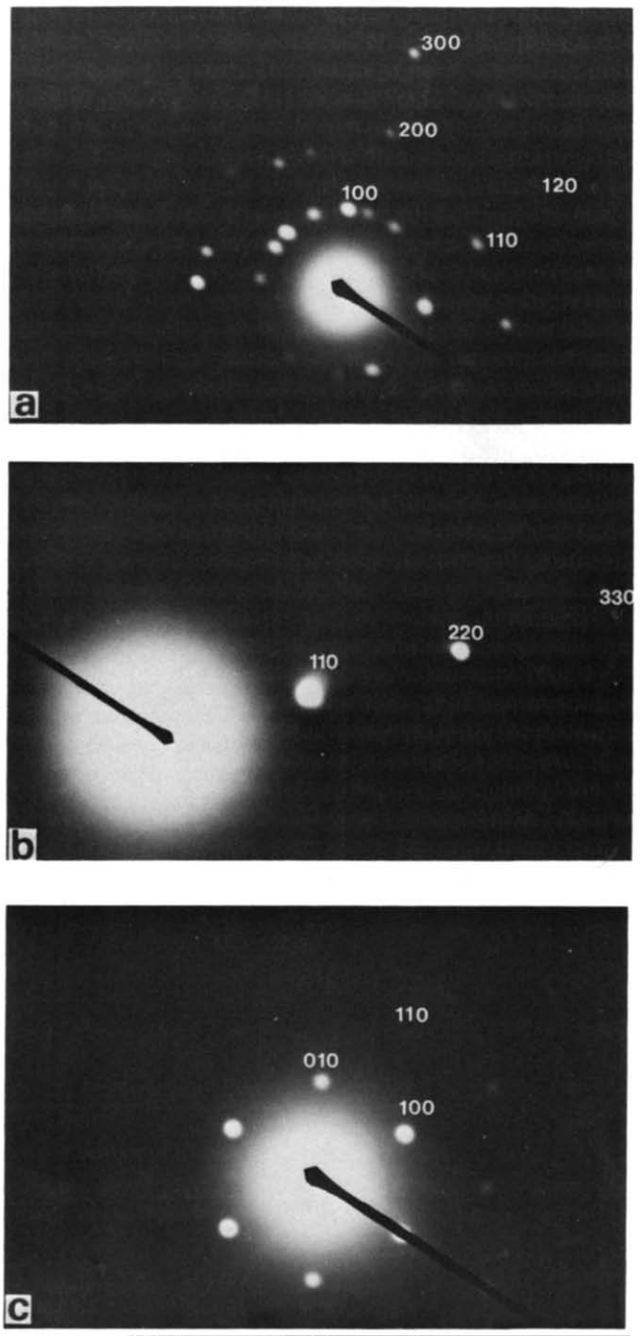

Figure 4 (a) diffraction pattern of a whole vesicle (*Figure 3a*), (b) diffraction pattern of a straight edge (*Figure 3b*), (c) diffraction pattern of a patch (*Figure 3c*)

$\beta_{\perp} = 1/N.a$; 10^{-2} Å$^{-1} < \beta_{\perp} < 2\text{–}10^{-2}$ Å^{-1}. The remaining part must be due to some paracrystalline disorder along the a axis. By microphotometry we measured the integral widths $\beta_{\parallel}(h)$ of simple reflections hoo on single domain patterns as in *Figure 4c*. When applying the ideal paracrystal theory of Hoseman and Bagchi[5]:

$$\beta_a^2(h) = \frac{1}{a^2}\left[\frac{1}{N_a^2} + \pi^4 g_a^4 h^4\right] + \beta_i^2$$

We found a distortion factor $g_a \simeq 7\%$ which represents the relative displacement from the normal period $a = 4.8$ Å.

Another striking fact we mentioned earlier is that when tilting a monocrystalline domain to an angle α to the electron beam the diffraction pattern does not disappear suddenly as should happen for a three dimensional perfect crystal. Along the 22 carbon atom chains there are, in the c direction, $N_c = 11$ lattice periods with $c = 2.54$ Å. Thus the hko reflections would be rods of integral width $\beta(c) = 1/c.N$; a 100 reflection should disappear for a tilting angle of $\alpha \sim 3°$. This is not the case as illustrated in *Figure 6a, b, c*, where the goniometer axis is parallel to [100]* and the tilt angles α are respectively 5°, 15° and 25°. When increasing the tilt, the pattern deforms as $1/\cos\alpha$, the circular spots become elliptic, the small axis being parallel to [100]*. The reciprocal space is composed therefore of cylindrical rods along the [001]* axis due to a paracrystalline disorder of the chains along c. By estimating the length of these rods, $\beta_c \sim 0.3$ Å^{-1}, the distortion factor along c is approximately $g_c = 25\text{–}30\%$. The fact that the chains have a high disorder along c and a small disorder along a is quite compatible with the point of view of compacity and may be interpreted from the packing of the chains in the unit cell. A translation of a chain along the a axis reaching 7% of the parameter $a = 4.8$ Å, forces the neighbouring chain to slide along the perpendicular c axis. This point is quantitatively discussed in the case of polyethylene crystals[6] where similar, but smaller distortions were found.

The distortions we measured here can be considered as intrinsic for crushed vesicles and not due to the electronic irradiation. Indeed, these microdiffraction spot breadth measurements take some 30 s at an intensity of 15 C/s m^2 so that the received dose 450 C/m^2 is far removed from the critical dose $D_c \sim 1 \times 10^4\text{–}2 \times 10^4$ C/m^2.

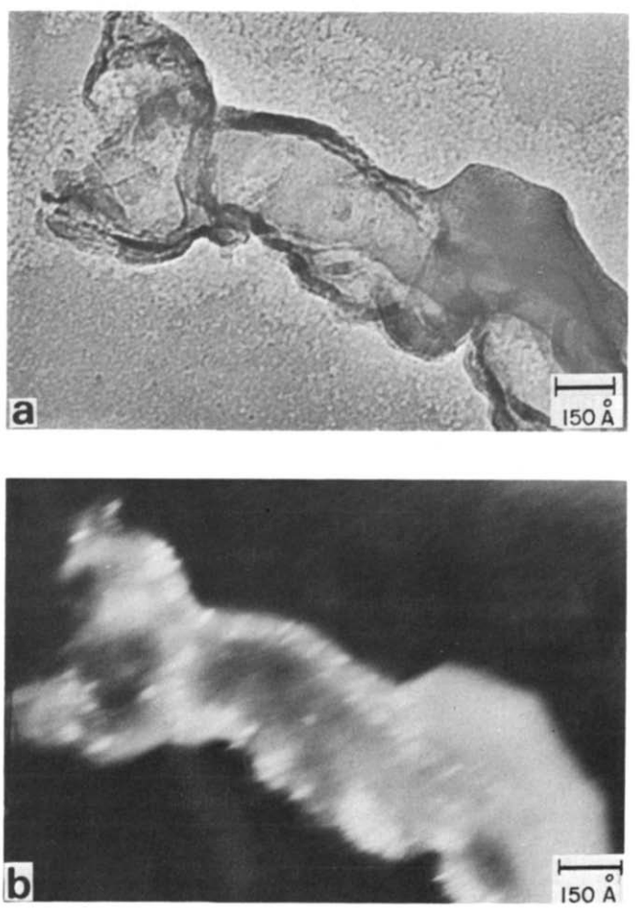

Figure 5 (a) bright field image of a crushed cylinder, (b) the same but in dark field with some 110 reflections

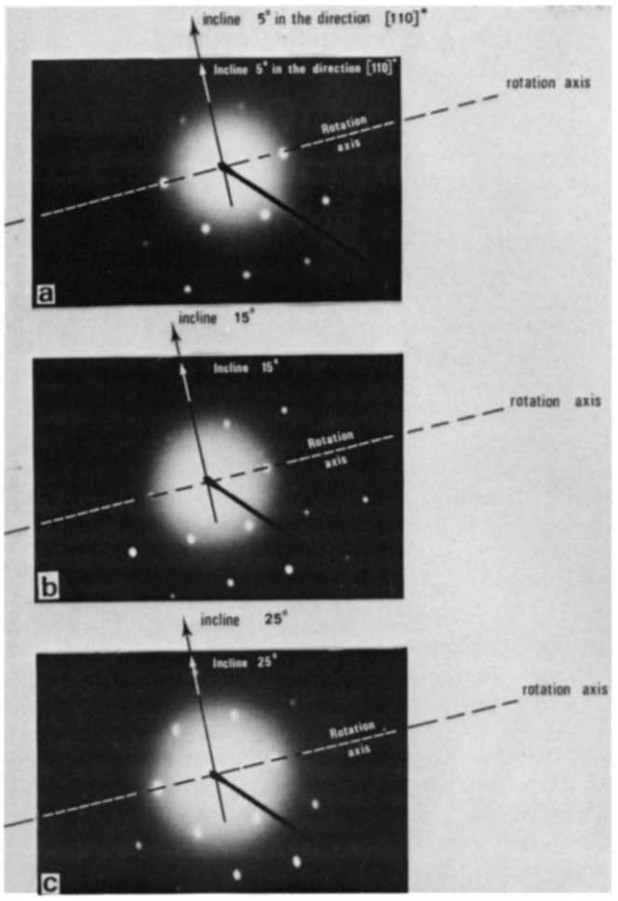

Figure 6 a,b,c: diffraction pattern of a monocrystalline patch as in *Figure 4c* but with different inclines in the direction |110|*. A sign of a pronounced two-dimensional character

STRUCTURE OF THE VESICLES AND THEIR GROWTH MECHANISM: DISCUSSION

Structure

In *Figure 7* we summarize schematically the different observations we made on crushed vesicles. The vesicles are formed by a monolayer membrane of 30 Å thickness, approximately the length of the lateral paraffin chains of the polymers. The surface of the vesicle is a mosaic of monocrystalline patches of ~50–100 Å where some 10^3 paraffin chains, normal to the surface, are hexagonally close packed with $a = 4.8$ Å as the shortest distance. These paraffin chains, inside each monocrystalline patch, show some paracrystalline disorder $g_a \sim 7\%$, $g_c \sim 25$–30%. The monocrystalline patches are mutually in azimuthal disorder forming grain boundaries.

On the border of a crushed vesicle the paraffin chains form bundles lying on the substrate with a period of 4.8 Å (see *Figure 7*). Sometimes these borders are straight so that the crushed vesicles (see *Figure 1d*) exhibit a polygonal contour.

From the above findings on crushed vesicles it is clear that the vesicles, when floating in the solvent, are closed spherical monolayer membranes with a thickness of 30 Å, so that the alkyl chains are close packed normally to the membrane. The oxygen of the ester groups, due to their van der Waals radii, can take part in this compact packing. The observed grain boundaries on the crushed vesicles may either be produced only during crushing or these boundaries may exist also in the non-crushed vesicles. In every case the vesicles must have defects since a sphere cannot be entirely paved with equilateral triangles. No experimental information is available on this point. Furthermore these monolayer membranes must be asymmetric, all the $-CH_3$ alkyl terminals are located on one face with the principal polymer chain running on the other face. Such an asymmetric membrane must have a natural curvature.

There are several pieces of evidence proving that the $-CH_3$ terminals are on the external surface of the vesicle while the ester groups and the principal chain of the polymer are located near the inner side of the vesicle. In *Figure 7b* is a schematic section of the polygonal shaped vesicles (as in *Figure 1d*). At the edges of the polygon, due to extreme curvature, there must be a splitting of the alkyl chain packing. Clearly the principal chain connecting two neighbouring alkyl chains must be located on the inner side of the vesicle since the links on the principal chain are very short ($x = 1$ in the formula of the copolymer, see section dealing with characterization of the copolymer). For a crushed vesicle (right hand side of *Figure 7b*) the same argument is pertinent.

Linking of monomers

We will now look at, in more detail, how the principal chain of the polymer is able to connect neighbouring lateral chains, which display hexagonal close packing. Each monomer has two bonds, one on the CH_2 group and another on the CH group of the principal chain as shown in *Figure 8* where a *trans*-configuration is represented, all carbon and oxygen atoms being in the plane of the drawing as well as the $-CH_2$ bond. The –CH bond which

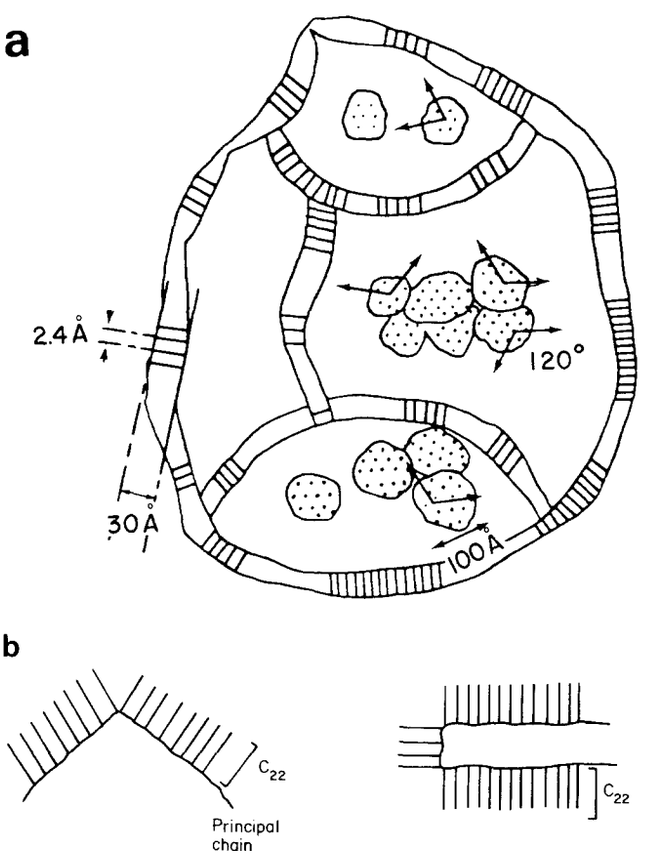

Figure 7 (a) Schematic structure model of a crushed vesicle; (b) schematic section of a polygonal vesicle and an edge of a crushed vesicle

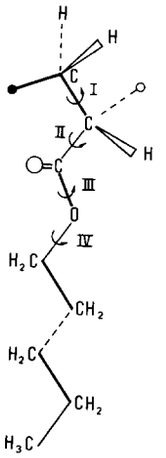

Figure 8 *Trans* configuration of a monomer unit

points outside this plane behaves differently. In the case of *Figure 8* the –CH bond points backwards and we shall call this case 0 and where the –CH bond points out from the paper will be called case 1. Notice that the free rotations around bonds I, II, III, IV transform the configuration to several others but none of them or their combinations are able to transform a monomer 1 to a 0 monomer, due to the 'asymmetric' character of the CH carbon. If we consider a second monomer which can either be of the same nature as the first one, so that the pair can be written as (0,0) or (1,1), or the second monomer may be of a different nature and written (0,1) or (1,0). When such monomers are engaged in a polymer chain and since there is no experimental mean to differentiate the ends of the chain, the symbols are arbitrary so that a pair can be called $i=(0,0)\equiv(1,1)$ (i: isotactic pair and $s=(1,0)\equiv(0,1)$ (s: syndiotactic pair).

In order to connect the elements of a pair, the CH bond of one element has to be matched with the CH_2 bond of the second element, the alkyl chains $0\text{—}(CH_2)_{21}CH_3$ having to remain in parallel orientation and remain at distances compatible with the translations of a hexagonal two-dimensional lattice with parameter $a=4.8$ Å. These translations can be easily found with the help of free rotating packing model molecules. For an isotactic pair as well for a syndiotactic pair the shortest distance can be approached can be seen in *Figure 9a, b, c*, when we look in particular at chains numbered monomer (1) and monomer (2). These translations can be described by $\vec{a}_i={}_0\vec{a}_0\equiv{}_1\vec{a}_1$ and $\vec{a}_s={}_0\vec{a}_1\equiv{}_1\vec{a}_0$ with $|\vec{a}_i|=|\vec{a}_s|=a$. But the connection can be made also for i and s pairs with greater distances involved, as can be seen in *Figure 9 d, e*, which is compatible with the hexagonal lattice. This connection is described by $\vec{b}_i={}_0\vec{b}_0={}_1\vec{b}_1$ and $\vec{b}_s={}_0\vec{b}_1\equiv{}_1\vec{b}_0$ with $|\vec{b}_1|=|\vec{b}_s|=a\sqrt{3}$. Greater distances than a and $a\sqrt{3}$ cannot be connected with monomers of the type considered here where only one CH_2 group is available.

Let us add and connect a third monomer on a preceeding pair. This is illustrated in *Figure 9 a, b, c*, where a third monomer labelled (3) is connected to the end of the vectors ${}_0\vec{a}_0$ and ${}_0\vec{a}_1$. *Figure 9a* shows a primary isotactic pair ${}_0\vec{a}_0$ and the resulting position ${}_0\vec{a}_{(0,1)}$. This additionnal vector has at its end point a monomer of either type 0 or type 1 since its CH dangling bond can have two orientations symmetric to its 0–0=C plane. This is a quite general feature for all primary pairs (1), (2) of *Figure 9a, b, c, d, d, e*, that the resulting pair has therefore a double endpoint index (0,1) meaning 0 or 1.

Notice also that the $a_1\vec{a}_1$ primary pair, rather than the $a_0\vec{a}_0$ pair gives, for the resulting monomer, a symmetrical position with respect to ${}_0\vec{a}_0$ (*Figure 9a*) since a plane of symmetry change alters monomer 0 to monomer 1. However, with the symbols 0 and 1 being arbitrary, there exists therefore, for any isotactic pair $\vec{a}_i={}_0\vec{a}_0\equiv{}_1\vec{a}_1$, two symmetrical backward ($2\pi/3$) first neighbour positions (*Figure 9a*) which are shown schematically in *Figure 10a*.

Choosing a primary syndiotactic pair as ${}_0\vec{a}_1$ in *Figure 9b* and *c*, there are two different non-symmetric positions for the third monomer, a forward ($\pi/3$) first neighbour position (*Figure 9b*) ${}_1a_{01}$ and a backward ($2\pi/3$) second neighbour position (*Figure 9c*) ${}_1\vec{b}_{01}$. Adding the symmetric possibility the building scheme is given in *Figure 10b*.

Furthermore a primary pair may be of *b* type. In *Figure 9d*, for an isotactic pair as ${}_0\vec{b}_0$, the resulting monomer is ${}_1\vec{a}_{01}$ in a forward ($\pi/6$) first neighbour position. For a syndiotactic pair as ${}_0\vec{b}_1$ (*Figure 9e*) the resulting monomer is ${}_1\vec{a}_{0,1}$ in a first neighbour right angle position. These two building schemes with their symmetrical alternatives are given in *Figure 10c* and *d*.

Growth mechanism

It must be verified that a two dimensional lattice can be built with a long principal chain which respects the exclusion rules just given. The growth of a two-dimensional crystal can be controlled by a diagram giving the total energy of an m molecule cluster as a function of its number of molecules m. The equilibrium form of the crystal is supposed to correspond to the lowest energy path on this diagram.

The energy diagram of a two dimensional paraffin crystal without connections between molecules is used as an example.

On a paraffin cluster in solution, the incoming molecules attach preferentially to the sites where they satisfy the greatest number of Van der Waals contacts. In order to be acquainted with this kind of diagram, an example of a two dimensional parrafin crystal is first considered. There are no covalent links between the different molecules in contrast to poly(alkylacrylate).

If ψ is the bond energy per such a contact between two alkyl chains, the potential energy of a molecule inside the cluster is $-6(\psi/2)$ and the energy of a molecule on a peripheral site j is $(-\psi_j)$ with $\psi<\psi_j<5\psi$.

The excess energy A_m of an m cluster with respect to an infinite cluster is:

$$A_m=3m\psi-\sum_{j=1}^{m}\psi_j$$

This quantity depends on the size and the form of the cluster. The minimal energy path for a paraffin crystal is drawn in *Figure 12* when its growth sequence is according to the numbers labelling the molecules in *Figure 11a*. The general envelope of A_m in *Figure 12* is proportional to $\sqrt{m}$ according to the Wulf theorem which is satisfied for each step.

When the alkyl molecules are linked together as in the polymer considered here there are two reasons why the same energy path cannot be followed: (1) an alkyl molecule cannot visit any peripheral site due to the short linking with its neighbouring molecule, (2) the alkyl

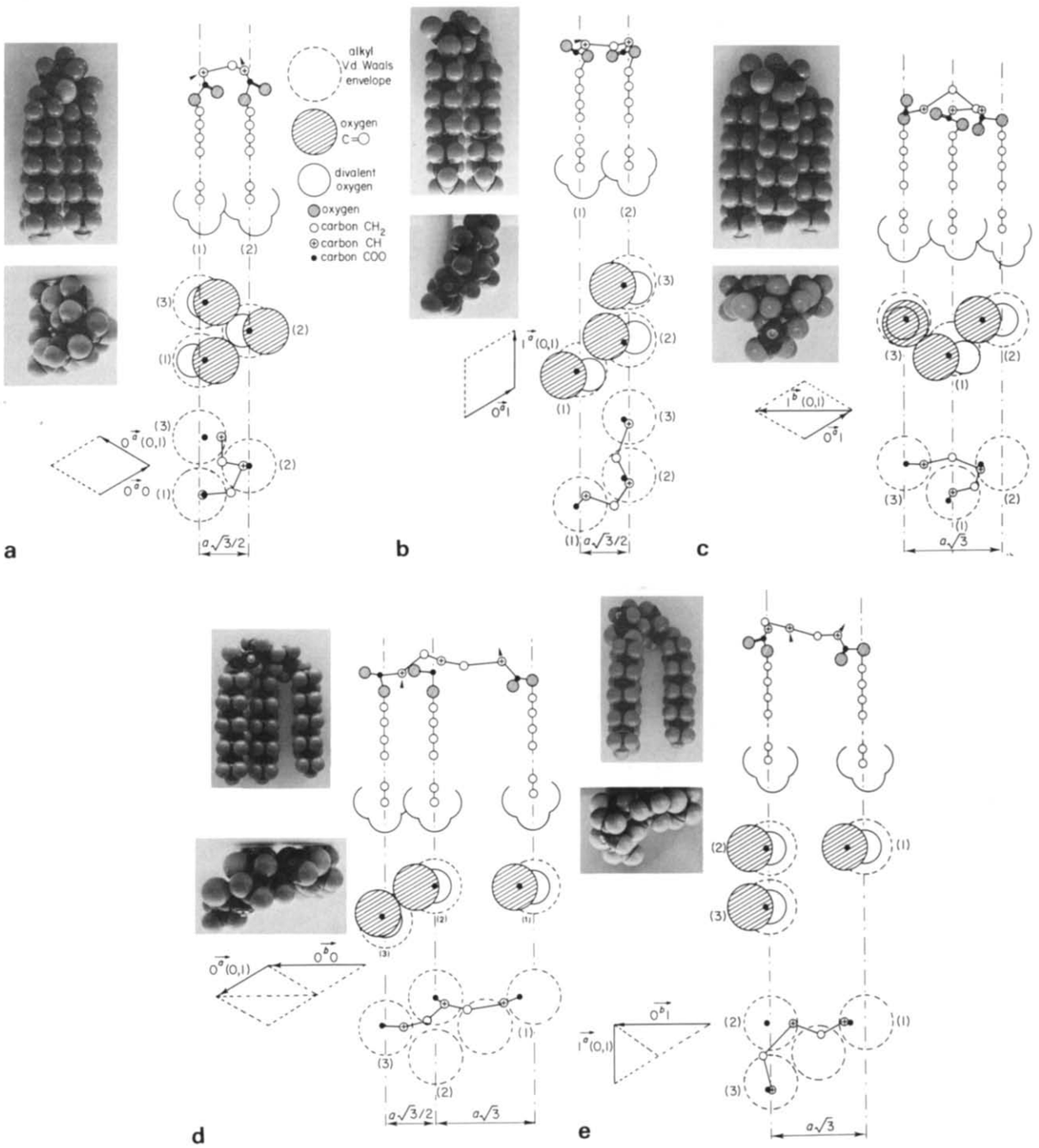

Figure 9 a,b,c,d,e: packing and linking of two and three monomer units of polyalkylacrylate

molecule has to obey the exclusion rules just given, so that it has not always the opportunity to choose the lowest energy site.

If we neglect the composition laws then reason (1) is the only constraint. In *Figure 11, b, c, d* different growth trajectories are followed by the polymer chain which would be located in *Figure 12*, above the minimal energy curve of the paraffin crystal. The total energies of the final crystals of *Figure 11 a, b, c, d*, are the same (identical size and forms) but during their growth history, different excited energy states appeared.

Coming to point (2) the growth mechanism of the polymer chain depends on its tacticity.

The growth of an isotactic chain leads to a linear zig zag morphology as in *Figure 13*, and the corresponding energy path follows the linear curve $A_m = 5\Psi - (m-2)\Psi$ when $m > 2$ but $A_1 = 3\Psi$. No excited states exist in this case.

For a syndiotactic chain, the composition laws (*Figure 10b. d*) make more sites available for the molecules than in the case of the isotactic sequence. Though satisfying the composition laws and the minimal energy path, in the crystallization of such a syndiotactic chain, four different clusters are built in *Figure 14a, b, c, d*. Their energy paths *Figure 12a, b, c, d* differ according to the choice of the composition laws at the very beginning of the clustering. These paths are located in between the isotactic energy path and the paraffin crystal path when the number of molecules is large.

Notice that a syndiotactic sequence gives, in every case, higher activation paths (*Figure 12*) than the isotactic

sequence. That means that in a long random suite of 0 and 1 symbols (atactic chains) nucleation has to take place in the sequence, where there is a local isotactic suite.

A random sequence of 200 monomers is taken as an example to build a crystalline domain of our poly-(alkylacrylate):

```
0 0 0 0 1 0 0 0 0 1 0 0 0 1 1 1 1 0 1 0 0 1 0 0 0 0 0 1 1 0 1 0 1
0 0 0 1 0 1 1 0 0 1 0 1 0 1 1 1 1 0 1 0 0 1 1 1 0 1 1 1 0 1 0 0 0 0 1 0
                  I
0 1 1 1 0 1 0 1 [0 0 0 0 0] 1 1 1 0 0 0 0 1 1 1 0 0 1 1 1 1 0 1 1 1 0 0
                                  II
1 1 0 1 1 0 0 1 1 0 1 0 1 0 1 0 1 0 1 0 0 0 1 [0 0 0 0 0] 1 1 0 1 1 1 0
  III
[1 1 1 1 1] 0 1 1 1 0 1 0 1 0 1 0 0 1 1 1 0 1 1 0 1 0 1 0 1 1 0 0 1 0 0
1 0 0 1 0 1 0 1 0 0 0 0 0
```

This sequence contains three isotactic suites of $m = 5$ at the points, I, II and III. *Figure 15* shows the minimal energy path structure obtained with only the nucleation centre I. Composition laws have been followed according to the sequence. The 0 and 1 symbols have been drawn in *Figure 15*, the arrows giving the sense of growth around nucleus I. One characteristic is that a two dimensionnal crystal is generated but holes are necessarily contained in it.

When two nucleation centres I and II grow simultaneously the resulting packing (see *Figure 16*) differs to that shown in *Figure 15*. There are two reasons for this:

(1) The growth proceeds independently from each nucleation centre I and II (see arrows near each centre) and the composition laws (*Figure 10*) are not all reversible with respect to symbols 0 and 1, and each nucleation centre builds its own structure.

(2) During shortening of the chain linking the centres I and II, both crystalline domains have coalesced by mutual rotation and a coherent grain boundary is generated. It also contains some holes. The arrows in *Figure 16* converge at a point M where the chain linking both centres is entirely crystallized. The growth boundary is coherent only when at point M a reversible composition law holds. When this condition is not satisfied, the resulting grain boundary is incoherent. When this coalescence is performed, the up to now non-crystallized chain on both opposite sides is able to find attachment sites along the neighbouring crystallization centre (see A and B in *Figure 16*) and finally they can cooperate.

DISCUSSION

What we wanted to show in the above discussion on

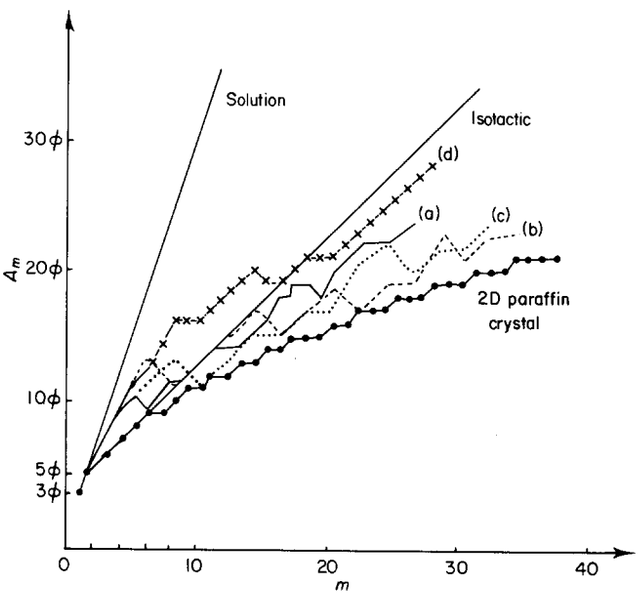

Figure 12 Energy path diagram (see text)

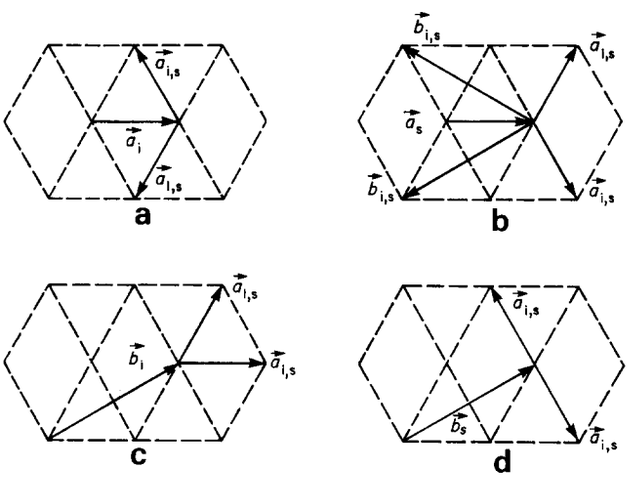

Figure 10 a,b,c,c: composition laws of three neighbouring monomers on an hexagonal lattice. In a and c, the two first monomers are an isotactic pair, in b and d, a syndiotactic pair

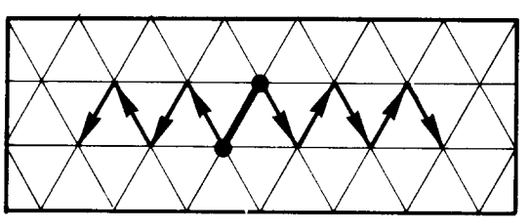

Figure 13 Minimal energy path structure for an isotactic sequence of polyalkyacrylate

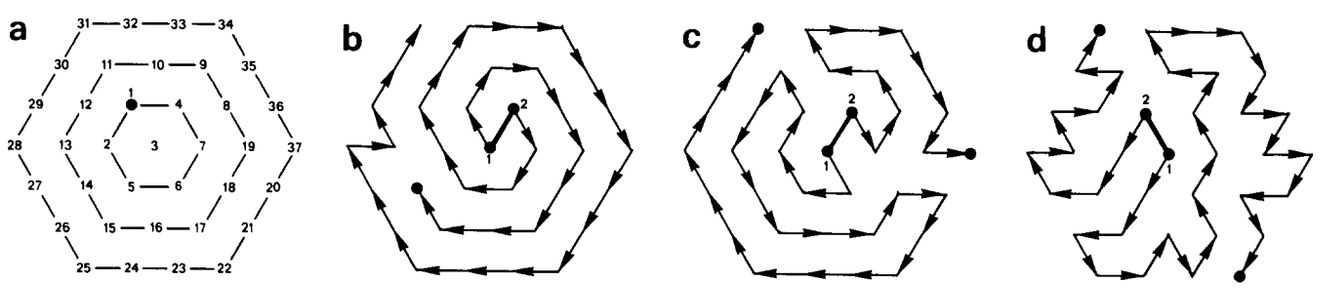

Figure 11 (a) hypothetical two-dimensional hexagonal paraffin crystal (see text); (b) the same as a, but chains linked on one side by a principal chain without steric constrains, minimal activation path structure; (c) the same as b but with higher activation path

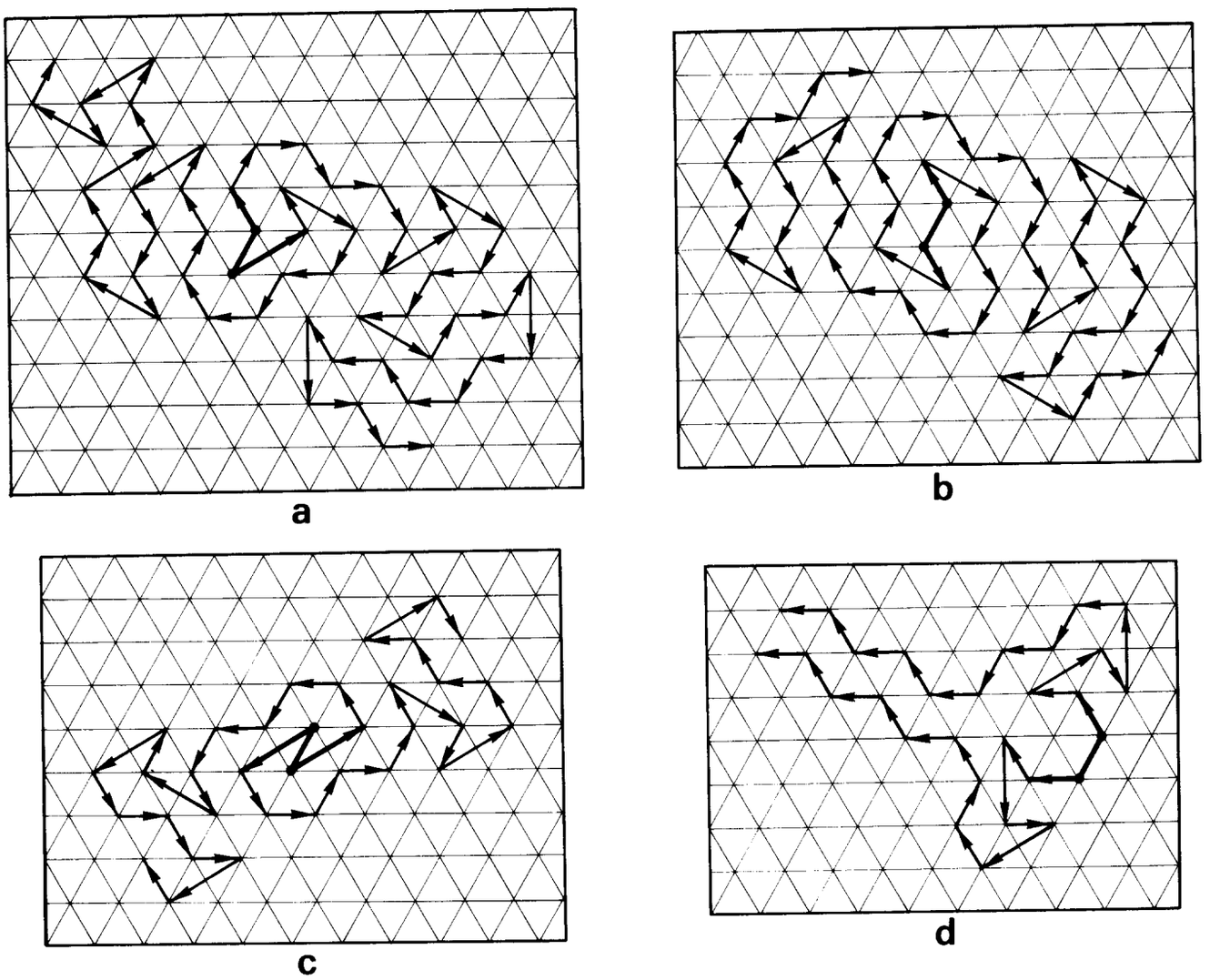

Figure 14 a,b,c,d: minimal energy path structures of a syndiotactic sequence of poly(alkylacrylate)

growth mechanisms is that the poly(alkylacrylate) is able to form a two dimensional hexagonal lattice particularly when the polymer sequence is atactic but this structure must necessarily contain holes. It may be that these holes are filled with solvent molecules. Isotactic local suites in the sequences are the most favorable nucleation centres. Their appearance in an atactic sequence is seldom enough and not too frequent so that crystalline domains of reasonable size can grow around them (for $m=5$ the frequency is $\sim 2.5\%$; $m=4$, $\sim 4\%$; $m=3$, $\sim 7\%$). Coalescence of these domains is quite possible in a coherent way (same hexagonal lattice) when neighbouring nucleation centres work simultaneously. Clearly, in spite of the coherence, holes are created. We build these membranes by following a minimal energy path. This corresponds to low growth rates as shown in *Figure 11b* for the special case of a polymer where linking of the alkyl chains are not constrained by composition laws. Clearly non equilibrium structures can also be obtained with the polymer considered here when rapid growth takes place. Such structures contain more internal boundaries and holes.

The congenital holes which are produced during the growth favour some fluctuation of parameter a of the hexagonal lattice. We found a paracrystalline disorder $g_a = 7\%$ which may be connected to this fluctuation and this results in a corresponding fluctuation along c (see section dealing with 'paracrystalline disorder'). It may be that this observed paracrystallinity is also due to the fact that the observed vesicles are crushed.

The hole and grain boundary formation is a fortunate situation since this two-dimensional lamellae have to curve in order to form closed vesicles. Indeed such defects are necessary since a sphere cannot be entirely paved by a regular triangular lattice having only six fold coordination.

From the foregoing, the length of the principal polymer chain determines the size of the crystalline patches of the vesicles or the maximal size of the vesicle when the molecular weight is sufficiently high.

Can different principal chains cooperate in order to form greater patches or vesicles? The answer is yes, in principle. Two isotactic nuclei each in its own principal chain, can come in contact and form a short ribbon, the non yet crystallized chains on their ends playing now mutually the attachment game. These chains form with the nuclei a boundary which has the property that no principal chain is crossing it. Therefore such a boundary may be fully separable without unwinding the chains as would be the case with the recently discussed coalescence

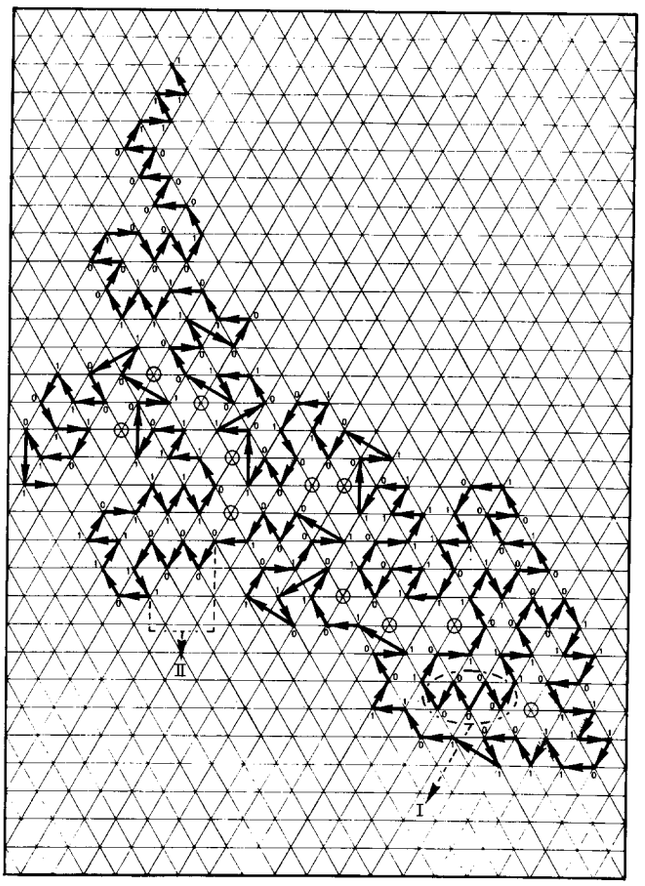

Figure 15 Minimal energy path structure of an atactic sequence when only one isotactic suite I works as nucleation centre

boundaries. This type of boundary may be the locus where vesicles can be definitively separable in a string of beads.

To say something pertinent about the mechanical properties of such monolayer membranes is risky. Due to the asymmetry of the monolayer the spontaneous curvature is quite secure. Due to the molecular holes resulting from the grow scheme, fluctuations of this curvature can be important. It may be guessed that the lateral elasticity of such membranes depends on these defects and that there is viscoelastic character being exhibited. Extrusion or ingestion of solvent molecules in the boundaries containing holes may contribute to the viscous behaviour. Notice also that such vesicles may have some permeability.

However, due to the linking by the principal chain, the monomers are hardly able to move in this type of membrane as they would in usual myelinic or natural membranes.

A last point we have to discuss in more detail concerns the necessary conditions for forming, with such polymers, closed lamellae or vesicles. In the section dealing with 'linking of monomers' we demonstrated that atacticity of the sequence belongs to one of the conditions. Are there conditions on the principal chain length or (and) the lateral alkyl chain length?

We tried crystallization experiments with atactic dodecylacrylate ($M_n = 5600$, $M_w = 14000$), using the same two-solvents technique* at 60°C. The atactic dodecylacrylate does not crystallize as closed membranes but produces lamellae of 300–1500 Å lateral extension. They are not crushed closed membranes since no peripheral edge of finite thickness is seen. Moiré patterns have been observed due to the superposition of lamellae and such lamellae give exactly the same diffraction patterns as those we described for C_{22} poly(alkylacrylate). When single lamellae are observed in bright field illumination with an aperture selecting the 100 spots, lattice images could be obtained. The smallest monocrystalline area being 60 Å in diameter and the biggest 200 Å. Neighbouring monocrystalline areas meet either in low or high angle boundaries. We will report in detail elsewhere about these observations.

According to the molecular weight of this C_{12} poly(alkylacrylate) there are some $m = 60$ alkylchains in a principal chain, so that the smallest crystalline patches in the lamellae contain several of them. In the case of C_{22} poly(alkylacrylate) the most probable value is $m \sim 200$ so that the observed domains (50–100 Å) in the crushed vesicles also contain one or several principal chains. Taking into account that in this case crushing divided some crystalline domains, the domains of C_{22} and C_{12} poly(alkylacrylates) are quite similar from their principal chain content. Molecular weight does not seem to determine the fact that in one case closed membranes are observed and in other they are not. Crystallization experiments have to be done at other temperatures and in particular with the C_{22} acrylates with well defined principal chains lengths.

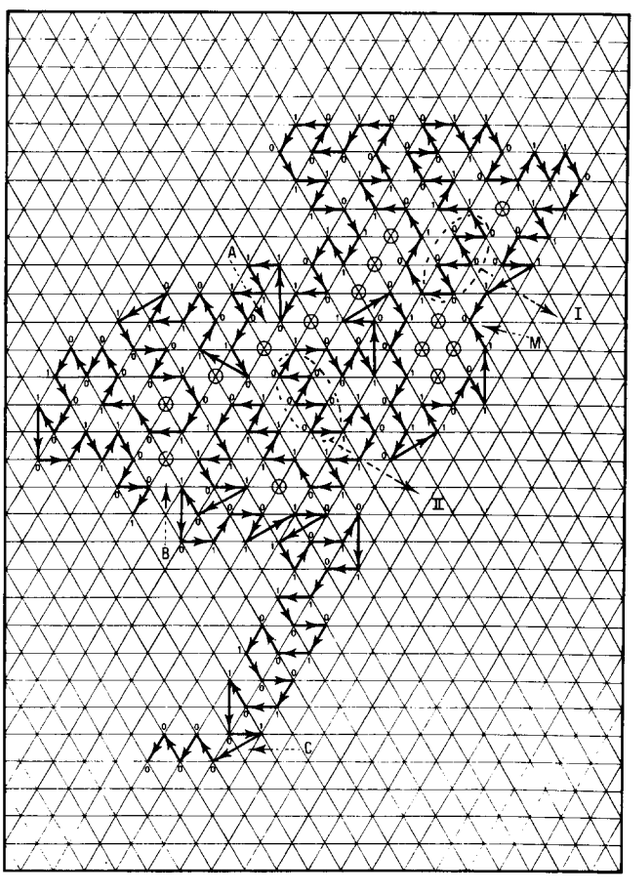

Figure 16 Minimal energy path structure of the same atactic sequence (as in *Figure 15*) when two isotactic suites, I and II, work as simultaneous nucleation centres

* According to (7) and (8) this polymer crystallizes from the melt as three-dimensional crystals, the alkyl chain being alternated on both sides of the principal chain in a plane

ACKNOWLEDGEMENTS

This work has been done in collaboration with the Compagnie Française de Raffinage. We thank them for some of the analytical results and a research Grant to one of us (S.G.). Drs J. Grosmangin, M. Marvillet, J. C. Petinelli of this Company helped with many stimulating discussions during this work. We had also fruitful discussions with Drs A. J. Kovacs, J. C. Wittmann and B. Lotz of the Centre de Recherches sur les Macromolécules of Strasbourg, Professor G. Vallet from Lyon kindly provided us with the samples.

REFERENCES

1 Nageotte, J., Morphologie des Gels Lipoïdes, Hermann et Cie. Paris (1937)
2 Saupe, A. *J. Colloïd Interface Sci.* 1977, **58**, 549
3 Wittmann, J. C., Candau, F., Kovacs, A. J. and Lotz, B. *J. Polym. Sci. Polym. Phys. Edn.*, 1982, **20**, 1341
4 Giorgio, S., *Thesis*, University Aix Marseilles III, July, 1983; Giorgio, S. and Kern, R. *J. Cryst. Growth*, 1983, **62**, 360
5 Kalendo, M. and Kasai, N. 'X-Ray Diffraction by Polymers', Kodansa Elsevier Pub. Company, p. 340 (1972)
6 Giorgio, S. and Kern, R. *J. Polym. Sci.* 1984, **22**, 1931
7 Plate, N. A. and Shibaev, V. P., *Polym. Sci. USSR*, 1971, **13**, (1) 466
8 Hsieh, H. W. S., Post, B. and Morawetz, H. *J. Polym. Sci., Polym. Phys. Edn.*, 1976, **14**, 1241